Acta Polytechnica **65**(3):349–360, 2025
https://doi.org/10.14311/AP.2025.65.0349

IMPACT OF PROCESS PARAMETERS ON THE MECHANICAL AND SURFACE PROPERTIES OF AA6082

Bilgehan Tunca[a,*], Bahadir Karaca[b]

[a] *Sistem Alüminyum, Department of R&D Center, Tekirdağ, Turkey*
[b] *Zahit Alüminyum, Department of R&D Center, Adana, Turkey*
[*] corresponding author: bilgehantnca@gmail.com

Abstract. This study investigates the effects of chemical composition, heat treatment, and processing parameters on the mechanical properties, microstructure, and surface quality of AA6082 aluminium alloy. Three castings with varying Mg and Si content were subjected to homogenisation at 580 °C for 8 and 10 hours, followed by extrusion and artificial ageing at 180 °C for 6, 8, and 10 hours, yielding 18 samples. Tensile testing, microstructural analysis, SEM examination, and anodic oxidation (18 V, 26–32 minutes) were conducted to assess performance. Results revealed that the highest tensile strength (361 MPa) and yield strength (332 MPa) were achieved with 8-hour homogenisation and ageing (B2 sample), attributed to optimal β'' precipitate formation, finer grain sizes, and a favourable composition (Mg: 0.92 %, Si: 1.09 %). The surface quality and hardness were enhanced by water shock and nitrogen gas cooling during extrusion, while the 10-hour homogenisation reduced porosity but increased the risk of over-ageing. SEM analysis confirmed ductile fracture in high-strength samples, and anodising produced thicker (11.7 µm), glossier coatings with longer processing times. These findings highlight the critical interplay of heat treatment duration, cooling strategies, and surface finishing in optimising AA6082 for industrial applications, with implications for process design and alloy development.

Keywords: Aluminium alloy, AA6082, heat treatment, aluminium casting, extrusion.

1. Introduction

The use of aluminium alloys is increasingly prevalent across various application areas due to their excellent physical and mechanical properties. Additionally, aluminium alloys, which are distinguished by their varying chemical compositions, are preferred in industrial applications for their superior machinability [1]. The improvement of their machinability and performance, tailored to specific application domains, has been extensively investigated within the framework of material improvement and development [2]. A critical aspect of the aluminium alloy production process involves determining the appropriate chemical composition based on the alloy specifications. Furthermore, heat treatment, conducted at varying temperatures and durations, plays an essential role in achieving a homogeneous microstructure. This heat treatment process directly influences extrusion capabilities and contributes to enhancing the mechanical properties of extruded aluminium profiles [3].

The 6XXX aluminium alloy series, defined as the Al-Mg-Si system, exhibits high fabricability. The chemical and microstructural composition of these alloys significantly impacts their functional properties and application suitability. Research has indicated that the mechanical properties of 6XXX-series aluminium alloys, subjected to heat treatment with T6 tempers, are strongly dependent on both the chemical composition and the ageing duration. In addition, the formation of β'' precipitates, which are closely linked to the hardness of aluminium alloys, increases with higher Mg and Si content in the alloy's chemical composition [4]. Numerous studies have focused on the effects of heat treatment and casting parameters on the mechanical and microstructural properties of aluminium alloys. It has been reported that intermetallic phases, such as Al-Fe, Al-Fe-Si, and Al-Fe-Mn-Si, with varying morphologies and physical properties, form depending on the casting conditions such as cooling rate and the alloy's chemical composition. Moreover, β-Mg_2Si phase precipitates, which are responsible for the strength of aluminium alloys, develop during cooling following the homogenisation [5].

Prabhukhot and Prasad (2015) [6] investigated the effect of heat treatment on the hardness of AA6082-T6 aluminium alloy. Artificial ageing was conducted at 175–220 °C for 2–10 hours, with some samples pretreated with solution heat treatment at 500 °C. Hardness was measured on the Rockwell E scale. Results showed that both processes altered the grain structure, reducing hardness, with brittle Mg_2Si phase increasing notably above 200 °C.

Ma et al. (2015) [7] examined the effect of solution heat treatment (SHT) on the mechanical properties and fracture behaviour of AA6082 aluminium alloy sheets. Using a central composite design, specimens underwent SHT at 440–575 °C for 1.7–58 minutes, followed by water quenching and artificial ageing at 190 °C for 3 hours. Tensile tests revealed that ultimate tensile strength (UTS) increased and ductility decreased with higher SHT temperatures and time. Response surface models were developed, and the NSGA-II algorithm optimised these parameters, showing UTS and ductility ranging between 201–252 MPa and 32–30 %, respectively, at 510–534 °C and 12–28 minutes. Scanning electron microscopy analysis indicated ductile fracture, with dimples becoming shallower as the SHT temperature and time increased.

Meredith et al. (2002) [8] investigated the intermetallic phase selection during the solidification of Al-Fe-Si(-Mg) alloys, focusing on 1XXX and 6XXX series compositions. Using directional solidification (20–120 mm min^{-1}) and varying Si (0.1–0.9 wt %) and Mg (0–3.5 wt %) content, they analysed phase transitions via microscopy, X-ray diffraction, and thermodynamic modelling. Results showed that increasing Si shifted phases from binary Al-Fe (e.g. Al_6Fe) to ternary Al-Fe-Si (e.g. α-AlFeSi, β-AlFeSi), while Mg (> 1.0 wt %) favoured Al_mFe and altered the primary aluminium morphology from columnar to dendritic, mirroring grain refiner (Al-Ti-B) effects. These shifts were linked to thermodynamic stability and kinetic factors, such as solidification velocity and primary phase morphology.

The formation of these intermetallic phases based on Fe content is directly affected by the cooling rate and the Fe to Si ratio in the matrix [9]. The Al-Mg responsible for precipitation hardening can be significantly improved by rapid solidification after the plastic deformation process. The hot extrusion process can be combined with rapid solidification for obtaining an aluminium profile with high mechanical properties [10]. The extrusion process, recognised as a form of plastic deformation, enables the transformation of an aluminium billet's dimensions under conditions of high temperature and high pressure. In this process, parameters, such as die temperature (°C), extrusion speed (mm s^{-1}), press pressure (bar), and press duration (s), are critical and significantly influence the extrusion performance of high-strength aluminium alloys. These parameters directly govern the alloy's shaping process and the mechanical properties of the final product. Precise adjustment of these factors is essential for aluminium alloy types containing different primary elements, as each alloy exhibits unique chemical compositions, flow characteristics, and melting behaviour [11].

The plastic deformation technique reveals that aluminium alloy groups with different chemical compositions exhibit distinct metal flow behaviour. For instance, an increase in extrusion temperature improves the alloy's fluidity and facilitating shaping, however, excessively high temperatures can lead to surface defects (e.g. hot cracking) or undesirable grain growth in the microstructure. Conversely, if the temperature is not high enough, the material loses fluidity, resulting in increased press pressure and potential die wear. On the one hand, raising the die temperature can reduce friction between the material and the die, yielding a smoother surface, however, if this temperature becomes excessive, the dimensional accuracy of the profile can be compromised. On the other hand, a decrease in die temperature hinders the flow and heightens the risk of surface scratches or shape irregularities.

When extrusion speed (mm s^{-1}) is increased, production pace may accelerate, however, excessively high speeds can cause inconsistencies in the flow and the development of internal stresses. If the speed is too low, the process duration extends, reducing energy efficiency. Elevating press pressure (bar) facilitates the shaping of harder alloys, however, this can impose excessive strain on the die, shortening its service life. The press duration (s) must align with other parameters; if too brief, shaping may remain incomplete, while if overly prolonged, it risks energy waste and material fatigue. Moreover, one of the key considerations is the precise control of material flow in high-strength aluminium alloys during extrusion, as this fundamentally determines both product quality and process effectiveness [12].

2. Material and methods

In this study, three different castings of the AA6082 alloy were performed. Subsequently, these three castings were subjected to homogenisation annealing processes at a constant temperature of 580 °C for 8 and 10 hours. As a result of these processes, six different samples were obtained. The samples were then put through an extrusion process to produce aluminium profiles. Afterwards, for the artificial ageing process, the profiles were kept in an environment with a constant temperature of 180 °C for three different durations: 6, 8, and 10 hours. Subsequently, the profiles underwent an anodising process for anodic oxidation coating. Throughout this process, a total of eighteen samples were produced. To examine the differences in the homogenisation process after casting, microstructure analyses were conducted on the billets. Following the artificial ageing process, tensile test samples from the profiles were analysed to investigate the differences. Finally, SEM analyses were performed to examine the coating following the anodic oxidation process.

2.1. Billet casting process

It has been reported that the chemical composition of a casting alloy and the casting parameters play a critical role in the formation of intermetallic phases within an aluminium matrix [8]. The casting process for the AA6082 aluminium alloy was carried out in induction furnaces. The chemical composition was analysed using a spectrometer. Aluminium billets with a diameter of 127 cm and a length of 80 cm were produced. Table 1 presents the chemical composition of AA6082 in accordance with standards. The chemical composition of the AA6082 aluminium alloy billets produced is provided in Table 2. The casting parameters used are detailed in Table 3.

Alloy	Si [%]	Fe [%]	Cu [%]	Mn [%]	Mg [%]	Cr [%]	Zn [%]
AA6082	0.7–1.3	0.50	0.10	0.40–1.0	0.6–1.2	0.25	0.20

Table 1. Standard chemical composition of AA6082.

Cast	Si [%]	Fe [%]	Cu [%]	Mn [%]	Mg [%]	Cr [%]	Zn [%]
A	1.03	0.32	0.11	0.37	0.90	0.21	0.16
B	1.09	0.39	0.12	0.37	0.92	0.227	0.15
C	1.10	0.46	0.10	0.40	0.89	0.22	0.09

Table 2. Chemical analysis of AA6082.

Cast	Melting temperature [°C]	Casting speed [mm s^{-1}]	Cooling water temp. [°C]
A	701	119	24
B	699	120	25
C	711	115	25

Table 3. Casting parameters of AA6082.

2.2. Heat treatment process

The 6XXX aluminium alloy series, defined as the Al-Mg-Si system, contains magnesium (Mg) and silicon (Si) as major elements. These key elements contribute to the formation of multiple phases. The multiphase structures that develop within the aluminium matrix influence the mechanical and physical properties of the alloy [13]. Solution heat treatment is recognised as the process responsible for the formation of precipitate phases in aluminium matrices. These precipitate phases directly affect the mechanical properties [5]. Heat treatment of AA6082 is typically conducted at a sub-eutectic temperature of 580 °C for a specific duration to promote the formation of precipitate phases in aluminium matrices [14]. Two different combinations of temperature and time were used during the heat treatment process. The parameters of the heat treatment process are provided in Table 4.

Temperature [°C]	Time [hour]
580	8
580	10

Table 4. Heat treatment of AA6082.

Şahbaz M. [15], has studied the effect of the change of microstructure and mechanical properties of AA6082 aluminium alloy. Different cooling processes were performed on the annealed aluminium billet samples. It was reported that the grain size decreases depending on the cooling rate after the heat treatment process. This decreasing of the grain size is directly related to the strength of the sample. Also, the type of phases formed in the aluminium matrix was affected by cooling rate and cooling type.

2.3. Extrusion process

One of the most critical factors in improving the surface quality and mechanical properties of aluminium profiles is the optimisation of extrusion process parameters, such as aluminium billet and die temperature (°C), extrusion speed (mm s^{-1}), and cooling conditions. These parameters are essential due to their role in continuously improving the microstructure. The extrusion process is typically conducted at temperatures between 500 °C and 520 °C [16]. Extrusion is also defined as a thermomechanical process that involves the application of high temperature and pressure. The temperature applied is crucial to ensure an isothermal extrusion process [17]. Table 5 presents the extrusion process parameters used.

Water shock cooling was also implemented during the extrusion process to enhance the mechanical properties of the aluminium profiles. It is well-known that water shock cooling directly influences the mechanical properties and surface quality of extruded aluminium profiles. Additionally, a nitrogen gas cooling system was used in the extrusion process of AA6082, with cooling channels positioned on the extrusion steel die. This cooling system helps to prevent uncontrolled oxidation on the surface of the aluminium profile.

2.4. Artificial ageing process

The ageing process is the final stage for improving the mechanical properties of the extruded aluminium profile. Table 6 shows the artificial ageing process parameters.

Alloy	Press [ton]	Billet length [mm]	Billet temperature [°C]	Die temperature [°C]	Press speed [mm s^{-1}]	Press pressure [bar]	Press time [s]	Cooling system
AA6082	2 500	540	480	450	3.7	210	132	on

Table 5. Extrusion process parameters.

Temperature [°C]	Time [hour]
180	6
180	8
180	10

Table 6. Artificial ageing parameters.

2.5. Anodic oxidation process

The efficacy of the extrusion process plays a critical role in determining the quality of the surface finishing process and the surface quality of the extruded aluminium profile. The anodic oxidation process, a surface finishing technique, is performed to induce a controlled form of oxidation on the aluminium surface. Anodic oxidation, also defined as an electrochemical process, utilizes various chemical solutions, voltage (V), and current (A). This process is widely used to improve aluminium surface quality and expand its use in industrial applications [18]. Table 7 presents the parameters of the anodic oxidation process.

At this stage, a pre-surface finishing process was conducted to prepare the aluminium surface for anodic oxidation. This pre-surface finishing process dissolves the uncontrolled oxide layer, which typically has a thickness of less than 1–2 µm [19]. Different anodic oxidation parameters were applied to investigate the thickness of the aluminium profile coating. The process parameters, specifically time and voltage, directly influence the thickness of the aluminium coating.

3. Results and discussion

3.1. Mechanical test

Mechanical tests were conducted on all samples with varying chemical compositions using a ZwickRoell machine with a capacity of 20 tonnes. Tensile strength, yield strength, and percentage elongation were determined. Three different chemical compositions were used in the production of the AA6082 series aluminium alloys. Additionally, each chemical composition was subjected to two distinct homogenisation processes, involving specific temperatures (°C) and durations (h. Subsequently, the homogenised samples were subjected to three different ageing processes, also defined by temperature (°C) and time (h). Mechanical testing was conducted on selected samples, with the reported values representing the mean of five measurements for each sample.

Table 8 presents the results of the mechanical test, with the highest tensile strength (Rm) of 361 MPa observed for sample B2. Several factors contribute to this superior performance, stemming from the combined effects of casting conditions, heat treatment parameters, and microstructural characteristics.

The chemical composition of Cast-B, from which B2 is derived, includes slightly higher Mg (0.92 %) and Si (1.09 %) contents compared to Cast-A (Mg: 0.90 %, Si: 1.03 %) and Cast-C (Mg: 0.89 %, Si: 1.10 %), as shown in Table 2. These elements are critical in the Al-Mg-Si system for forming β'' (Mg_2Si) precipitates, which improve precipitation hardening and thus contribute to strength. Although the compositional differences are subtle, they likely provided a marginal advantage in strengthening B2. Additionally, the casting parameters for Cast-B (Table 3) reveal a higher casting speed (120 mm s^{-1}) and a lower pouring temperature (699 °C) compared to Cast-A (119 mm s^{-1}, 701 °C) and Cast-C (115 mm s^{-1}, 711 °C). The elevated casting speed likely reduced solidification time, promoting finer grain sizes, which are known to increase strength according to the Hall-Petch relationship. The lower pouring temperature may have further prevented excessive grain growth, optimising the microstructure.

The homogenisation process for B2, conducted at 580 °C for 8 hours, appears to have struck an optimal balance. In contrast, samples subjected to 10-hour homogenisation (e.g. B4–B6) consistently exhibited lower tensile strengths (e.g. B6: 313 MPa), possibly due to over-ageing or coarsening of precipitates. This suggests that the 8-hour duration preserved the size and distribution of β'' precipitates effectively. Similarly, the artificial ageing process at 180 °C for 8 hours produced ideal conditions for precipitation hardening. Samples aged for 6 hours (e.g. B1: 298 MPa) showed insufficient hardening, while those aged for 10 hours (e.g. B3: 351 MPa) approached but did not surpass B2, indicating that 8 hours is optimal for precipitate formation without leading to over-ageing.

Microstructural analysis (Section 3.2) further supports these findings, as B2 exhibited smaller, more homogenised grain sizes and fewer inclusions compared to samples such as A1, C1, and C2. The rapid water shock cooling and nitrogen gas cooling applied during extrusion (Table 5) likely enhanced this effect by maintaining precipitate solubility and promoting a refined microstructure, which translated into superior mechanical properties during ageing.

In summary, the highest tensile strength of 361 MPa in B2 is attributed to a synergy of factors: a slightly

Solution [g L^{-1}]	Voltage [V]	Time [minutes]
180 g L^{-1} sulfuric acid (H_2SO_4)	18	26
180 g L^{-1} sulfuric acid (H_2SO_4)	18	32

Table 7. Anodic oxidation parameters.

Samples	Homogenization parameters [°C − hour]	Hardness [HB]	Aging parameters [°C − hour]	Yield strength $R_{p0.2}$ [MPa]	Tensile strength R_m [MPa]	Elongation [%]
A1	580 °C – 8 h	103	180 °C – 6 h	308	331	11.5
A2	580 °C – 8 h	103	180 °C – 8 h	319	342	12.6
A3	580 °C – 8 h	103	180 °C – 10 h	307	318	10.4
A4	580 °C – 10 h	105	180 °C – 6 h	292	309	9.7
A5	580 °C – 10 h	105	180 °C – 8 h	288	304	9.2
A6	580 °C – 10 h	105	180 °C – 10 h	272	296	9.1
B1	580 °C – 8 h	103	180 °C – 6 h	281	298	9.3
B2	580 °C – 8 h	103	180 °C – 8 h	321	361	13.0
B3	580 °C – 8 h	103	180 °C – 10 h	332	351	12.8
B4	580 °C – 10 h	105	180 °C – 6 h	292	311	9.6
B5	580 °C – 10 h	105	180 °C – 8 h	284	318	9.9
B6	580 °C – 10 h	105	180 °C – 10 h	292	313	9.6
C1	580 °C – 8 h	103	180 °C – 6 h	317	322	10.3
C2	580 °C – 8 h	103	180 °C – 8 h	299	319	9.9
C3	580 °C – 8 h	103	180 °C – 10 h	287	307	9.4
C4	580 °C – 10 h	105	180 °C – 6 h	288	302	9.4
C5	580 °C – 10 h	105	180 °C – 8 h	272	296	9.1
C6	580 °C – 10 h	105	180 °C – 10 h	267	289	8.9

Table 8. Mechanical test results.

favourable chemical composition, a higher casting speed leading to finer grains, an 8-hour homogenisation process preventing precipitate coarsening, and an 8-hour ageing process optimising β'' precipitate formation. These conditions collectively outperformed other samples, such as A2 (342 MPa) and B3 (351 MPa), where variations in casting speed or ageing duration were less optimal, and C-series samples, which suffered from slower casting speeds and larger grain sizes.

Chen et al. [20] reported that 6XXX series aluminium alloys tend to exhibit lower strain rate sensitivity compared to 7XXX series aluminium alloys. Heat treatment directly affects the mechanical properties of aluminium alloys. Oosterkamp et al. [21] found that AA6082, in T6 and T79 temper conditions, displayed low strain rate sensitivity. Jadhav et al. [22] investigated the effect of various artificial ageing temperatures (ranging from 150 °C to 210 °C) on the mechanical properties of AA6082. Their study reported that the peak strength was achieved at a temperature of 170 °C.

3.2. Microstructure analysis

The microstructures and grain sizes of the six samples exhibiting the highest tensile test results were analysed. For the microstructural analysis, the samples were not etched, whereas etching was performed for grain size evaluation. All microstructure images were observed at 100× magnification. Grain size examinations were conducted at various magnifications. Figure 1 presents the images of samples A1, A2, and B2, while Figure 2 displays the images of samples B3, C1, and C2.

In the sample examinations, grain sizes between 110 and 205 µm were examined. The best results were obtained for samples A2, B2 and B3. Inclusion formations in their microstructures are lower than in the other three samples (A1, C1 and C2) and grain sizes are more homogenised and smaller. Figure 3 shows the grain size.

When examining grain sizes, a significant difference was observed between samples A2 and C2. A detailed analysis suggests several potential reasons for this disparity. Firstly, when the homogenisation process parameters – temperature and duration – were evaluated, both appeared consistent and identical for the two samples. This indicates that the homogenisation conditions are unlikely to directly contribute to the observed variation in grain size. Similarly, an analysis of the chemical compositions, measured using spectroscopic techniques (e.g. XRF or ICP-OES), revealed no significant differences in elemental content, suggesting

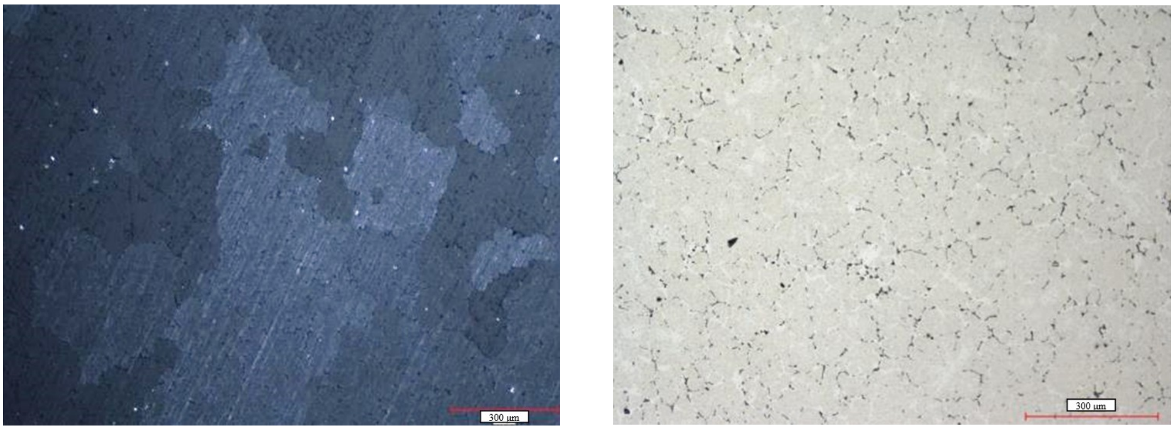

(a). Structures of sample A1.

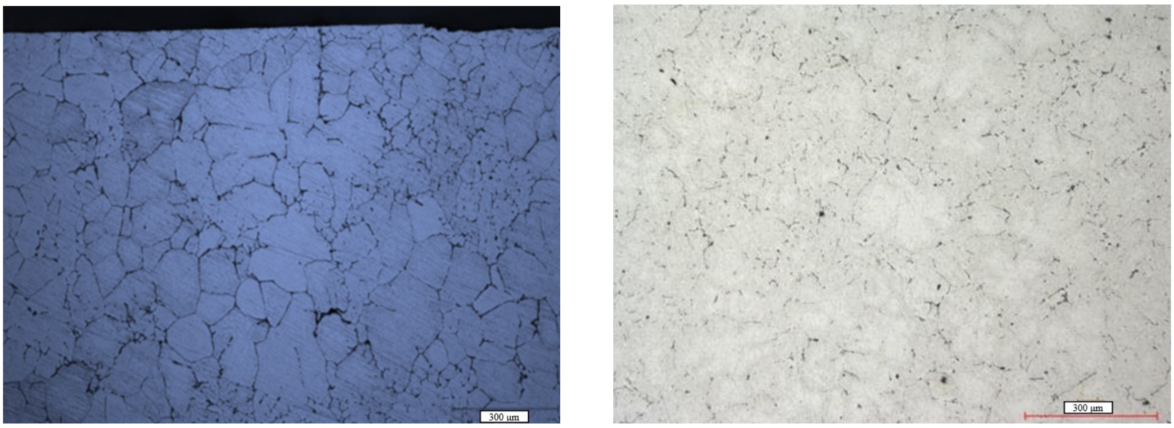

(b). Structures of sample A2.

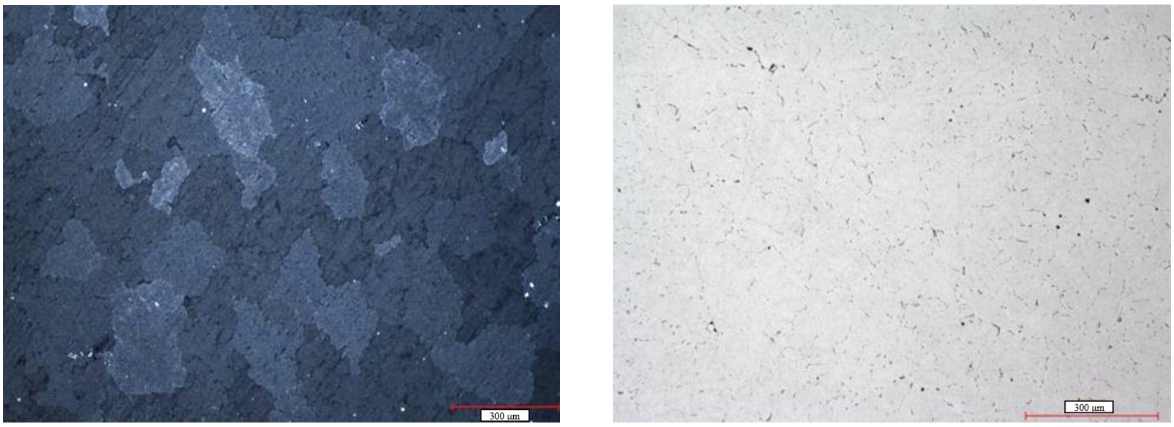

(c). Structures of sample B2.

Figure 1. Microstructure and grain sizes of the samples.

that the chemical composition alone cannot account for the observed discrepancy.

However, more pronounced clues emerge when examining the casting conditions. The C2 sample, associated with the Cast-C process, had a pouring temperature of 711 °C, which is lower than that of the Cast-A and Cast-B processes. Furthermore, the casting speed for Cast-C was observed lower compared to the other two casting processes (Cast-A and Cast-B). It is well-established that parameters such as casting speed and temperature directly influence the solidification kinetics and microstructure formation of liquid metal. Specifically, a lower casting speed extends the solidification time, potentially promoting grain growth, as slower cooling rates allow more time for dendritic structures to develop. Indeed, the grain sizes of samples from Cast-A and Cast-B were observed to be smaller than those of Cast-C, supporting the hypothesis that differences in casting conditions impact grain size.

Nevertheless, casting conditions alone may not fully explain this variation. The possibility of a localised

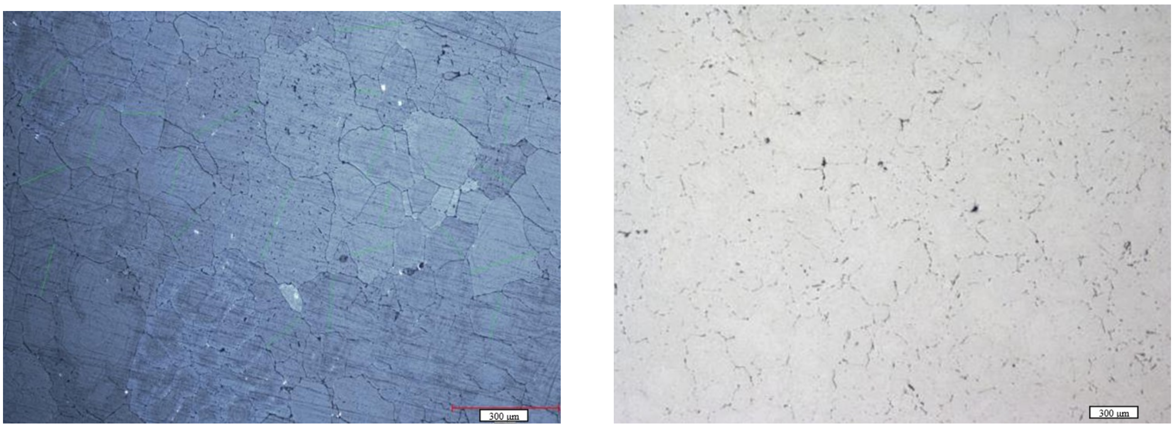

(a). Structures of sample B3.

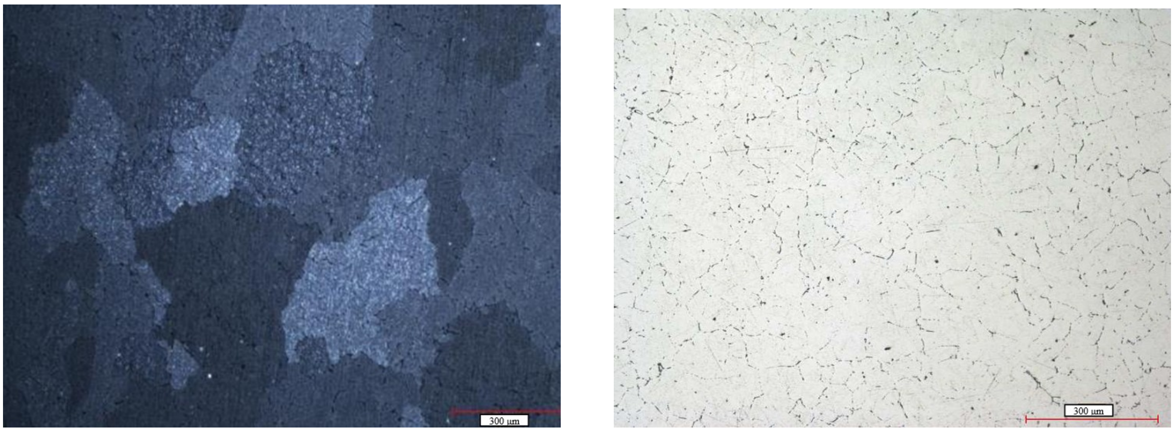

(b). Structures of sample C1.

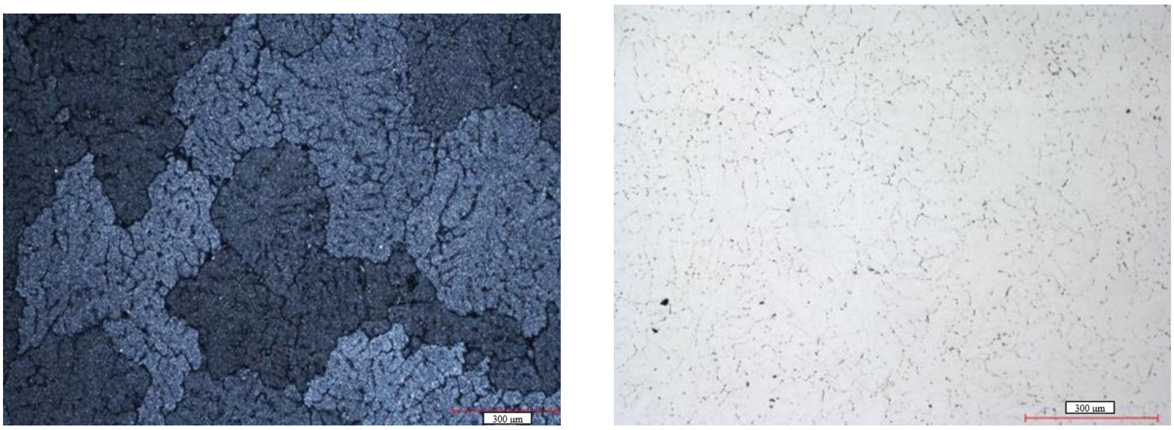

(c). Structures of sample C2.

Figure 2. Microstructure and grain sizes of the samples.

temperature increase during casting should not be overlooked. For instance, irregularities in the molten metal's flow dynamics within the mould or an uncontrolled rise in mould temperature could lead to uneven advancement of the solidification front, resulting in grain size heterogeneity. Additionally, a reduction in the amount of AlTiB (Aluminium-Titanium-Boron) alloy used as a grain refiner may have contributed to this effect. AlTiB facilitates grain refinement by providing TiB_2 particles that act as nucleation sites within the molten metal. If the AlTiB dosage in the C2 sample's casting was insufficient or inadequately distributed, this could have resulted in larger grain sizes. Verifying this hypothesis would require monitoring the AlTiB dosage and its mixing homogeneity during the process.

In conclusion, while variations in casting temperature and speed appear to be the primary contributors to the grain size differences, factors such as temperature fluctuations and potential deficiencies in grain refiner quantity should also be considered. For future studies, a systematic experimental design is recom-

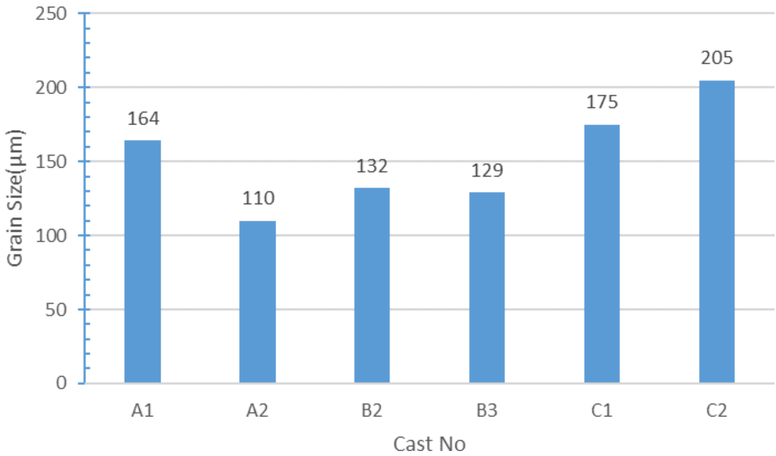

Figure 3. Graph of grain size.

mended to control and optimise these parameters comprehensively. For example, casting temperature could be incrementally increased from 700 °C to 750 °C, casting speed could be tested at varying flow rates, and AlTiB dosage (e.g. from 0.5 kg ton^{-1} to 2 kg ton^{-1}) could be systematically adjusted, with its impact on grain size analysed using statistical methods such as ANOVA. Furthermore, advanced microstructural characterisation techniques, such as optical microscopy or EBSD (Electron Backscatter Diffraction), could be used to provide a more detailed examination of grain size distribution and crystallographic orientation. Such an approach would establish a more precise relationship between process parameters and grain size outcomes.

3.3. SEM analysis

SEM analysis was conducted to investigate the surface characteristics following the homogenisation heat treatment. The analysis was performed on samples A2, B2, and B3, which exhibited superior mechanical properties. Figure 4 presents SEM images of these different samples. Figure 5 displays the SEM analysis of the anodic oxidation surface. The examinations were carried out using an FEI Quanta 650 Field Emission SEM under vacuum conditions at various magnifications at the Çukurova University Central Research Laboratory. Additionally, SEM analysis was performed to examine the fracture surfaces of these samples.

When a comparative analysis of SEM (Scanning Electron Microscopy) images was conducted, it was clearly observed that the fracture surface of the B3 casting sample exhibits a significantly more ductile microstructure than the other SEM images analysed. This ductile character is evident from the presence of pronounced plastic deformation traces on the fracture surface and the predominance of microscopic features typically associated with ductile fracture such as dimple formations. In contrast to the other samples, this distinction in the fracture surface of B3 reflects a variation in the material's mechanical behaviour. Consequently, it can be predicted that this ductile behaviour is directly related to the material's key mechanical properties, such as toughness and strength. Specifically, a ductile microstructure generally indicates a higher energy absorption capacity and the ability of the material to undergo greater deformation prior to fracture, suggesting that the B3 sample may possess superior fracture toughness compared to the others. The underlying reasons for this difference could stem from factors, such as casting conditions, chemical composition, or heat treatment parameters, warranting a more detailed investigation to elucidate the contributing factors.

4. Conclusion

This study explored the influence of chemical composition and heat treatment processes on the mechanical and microstructural properties of AA6082 aluminium alloy, with a focus on optimising these properties for industrial applications. Three distinct chemical compositions were subjected to homogenisation heat treatment at 580 °C for 8 and 10 hours, followed by artificial ageing at 180 °C for 6, 8, and 10 hours. The resulting 18 samples were analysed through tensile testing, microstructural examination, SEM analysis, and anodic oxidation assessments to evaluate the effects of these parameters. Additionally, the anodising process was conducted with two sets of parameters (18 V for 26 and 32 minutes) to investigate the quality of the surface coating.

The mechanical test results demonstrated that the highest tensile strength (361 MPa) and yield strength (332 MPa) were achieved for samples A2, B2, and B3, with B2 exhibiting the peak tensile strength after 8 hours of homogenisation at 580 °C and 8 hours of ageing at 180 °C. This superior performance is attributed to a synergy of factors, including a slightly elevated Mg (0.92 %) and Si (1.09 %) content in Cast-B, a higher casting speed (120 mm s^{-1}), and a lower pouring temperature (699 °C), which promoted finer grain sizes and optimal β'' (Mg_2Si) precipitate distribution. In contrast, samples homogenised for 10 hours

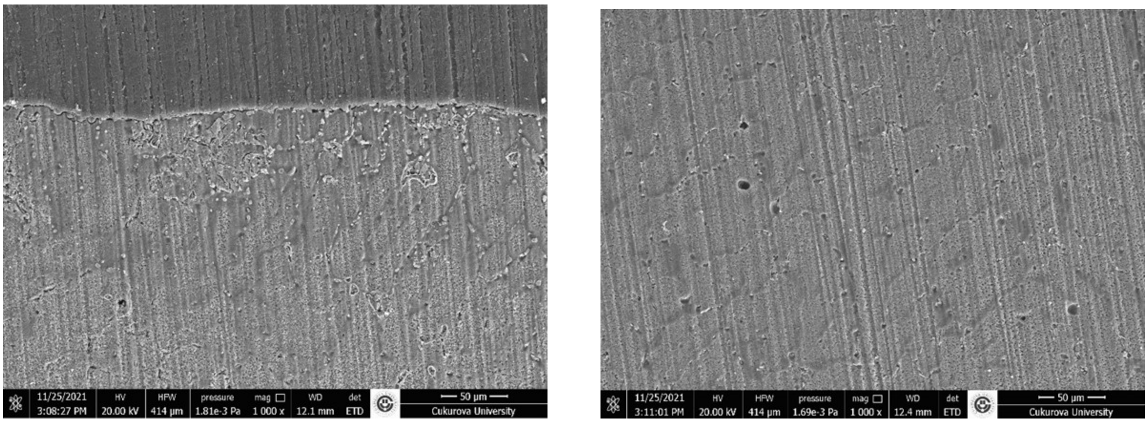

(a). SEM images of the A2 sample.

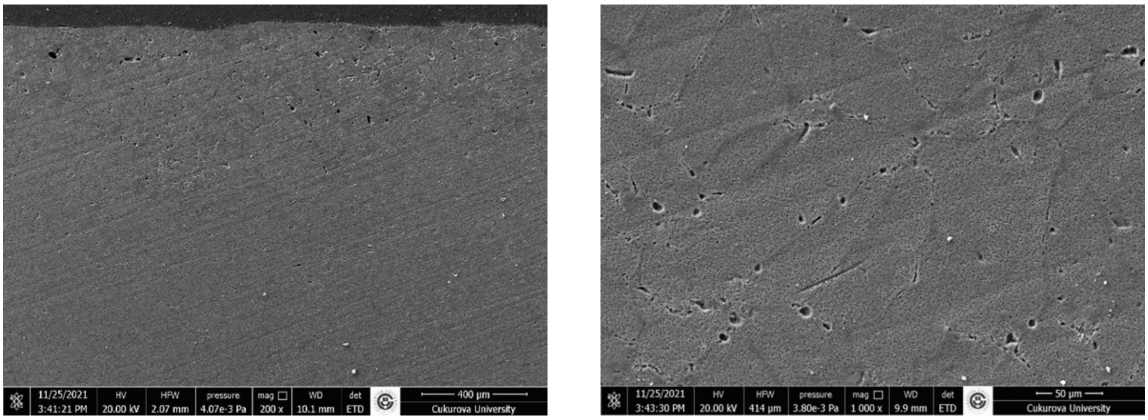

(b). SEM images of the B2 sample.

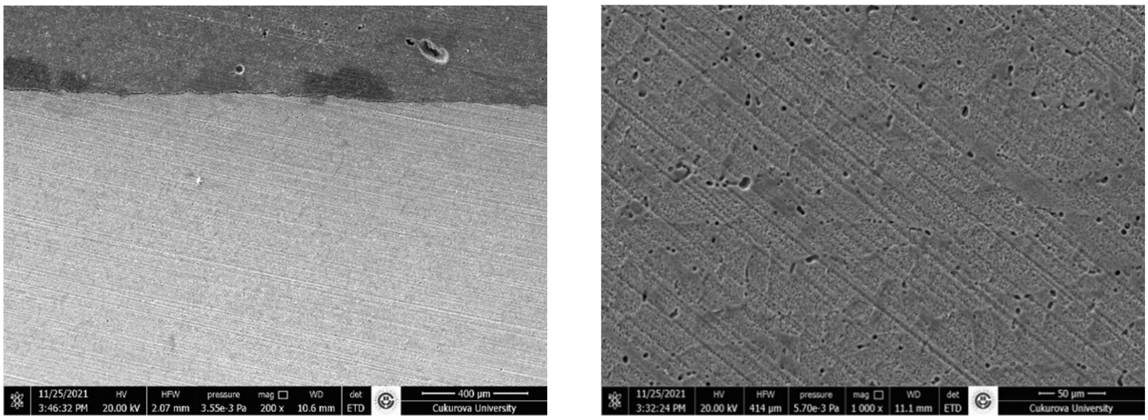

(c). SEM images of the B3 sample.

Figure 4. SEM images of the samples.

showed reduced strength, likely due to over-ageing, while the 8-hour homogenisation and ageing durations struck an ideal balance for precipitation hardening. Microstructural analysis revealed that the 10-hour homogenisation process resulted in fewer shrinkage gaps along grain boundaries and reduced surface porosity compared to the 8-hour treatment, indicating improved microstructural homogeneity with extended heat treatment time.

The extrusion process, improved by direct water shock cooling, positively impacted surface quality and hardness. Post-extrusion surfaces exhibited a smoother, more homogeneous texture, attributed to rapid cooling that preserved precipitate solubility and refined the microstructure. The use of a nitrogen gas cooling system during the extrusion further reduced thermal fatigue in the die steels, despite their high thermal conductivity, thereby improving surface quality and extending the die longevity. These findings underscore the critical role of cooling strategies in achieving high-quality aluminium profiles.

The SEM analysis of the fracture surfaces revealed that samples with the highest mechanical properties, such as B3 (yield strength: 332 MPa), exhibited more

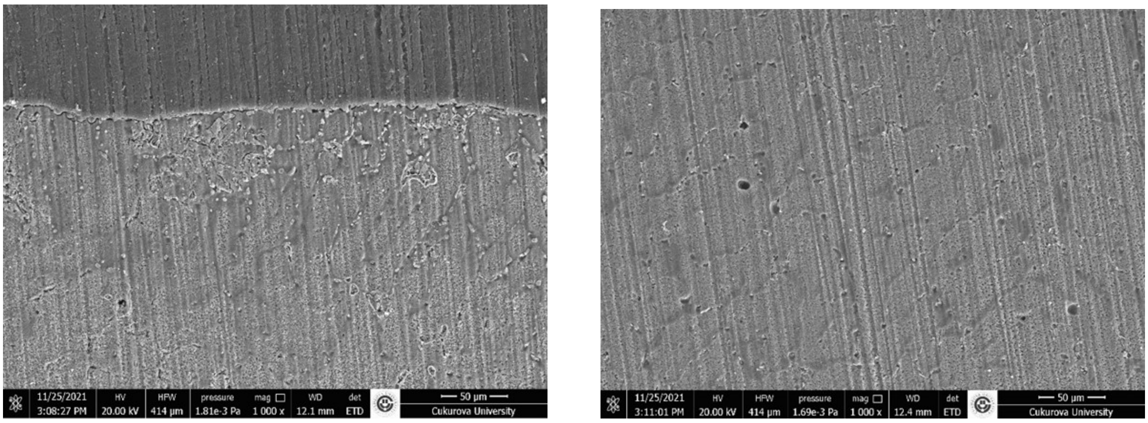

(a). SEM images of the A2 sample.

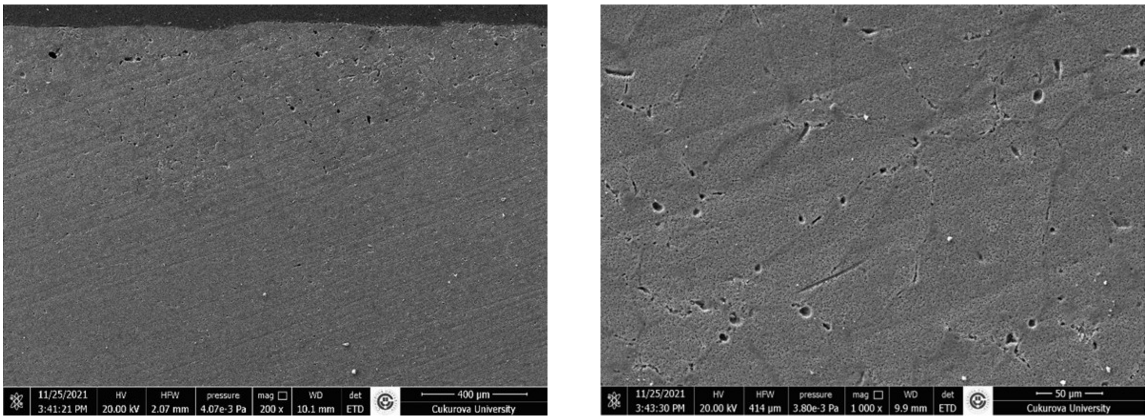

(b). SEM images of the B2 sample.

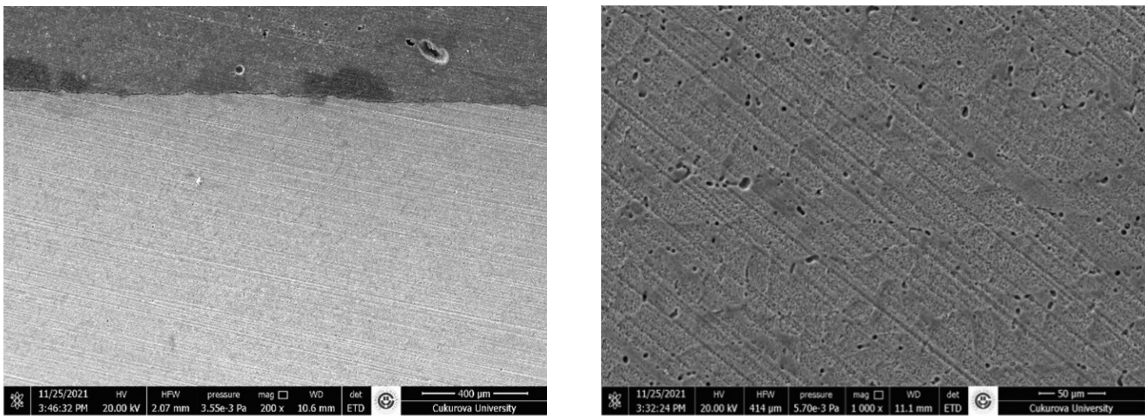

(c). SEM images of the B3 sample.

Figure 5. SEM images of the anodic oxidised surfaces of samples.

ductile behaviour, characterised by less dense fibrous structures and wider grain size distributions. This ductility correlates with improved toughness, influenced by the temperature and duration of the homogenisation process, which directly shaped the grain structure and precipitate morphology. Conversely, samples with shorter ageing times (e.g. 6 hours) showed insufficient hardening, while prolonged ageing (10 hours) risked over-ageing, highlighting the need for a precise parameter control.

The anodizing process, leveraging aluminium's natural oxide-forming tendency, produced controlled oxide layers with thicknesses ranging from 10.6 to 11.7 µm and improved gloss. The thickest and brightest coatings were achieved at 18 V for 32 minutes, particularly for samples homogenised at 580 °C for 8 hours and aged at 180 °C for 8 hours (e.g. B2). This suggests that the homogenisation and ageing processes not only enhance mechanical properties but also influence the surface treatment quality, likely by affecting the alloy's surface reactivity and microstructure prior to anodising. The coating thicknesses and gloss of the samples as a result of the anodic oxidation process are given in Table 9.

Sample	Homogenization Parameters [°C – h]	Aging Parameters [°C – h]	Voltage [V]	Time [minutes]	Coating Thickness [µm]	Gloss
A2	580 °C-8 h	180°C-8 h	18	26	10.8	53
				32	11.4	54
B2	580 °C-8 h	180 °C-8 h	18	26	10.6	51
				32	11.6	55
B3	580 °C-8 h	180 °C-10 h	18	26	10.9	52
				32	11.7	57

TABLE 9. Anodic oxidation results.

In summary, the mechanical properties, microstructural integrity, and surface quality of AA6082 aluminium alloy are governed by a complex interplay of chemical composition, heat treatment duration, cooling techniques, and anodising parameters. The optimal conditions identified, which are 8-hour homogenisation at 580 °C, 8-hour ageing at 180 °C, and rapid cooling during the extrusion, yielded the highest strength (361 MPa) and ductility, as observed for B2, while also supporting superior anodic coating. Future research could further refine these outcomes by systematically varying casting and cooling parameters, exploring grain refiner effects (e.g. AlTiB dosage), and using advanced techniques such as EBSD to deepen the understanding of microstructural evolution. These advancements could significantly improve the performance of high-strength aluminium profiles in industrial applications.

Key takeaways

(1.) Optimal Heat Treatment Parameters: Homogenisation at 580 °C for 8 hours followed by artificial ageing at 180 °C for 8 hours yielded the highest mechanical properties for AA6082, with a peak tensile strength of 361 MPa (B2 sample), demonstrating the importance of balanced heat treatment durations to maximise precipitation hardening without over-ageing.

(2.) Influence of Chemical Composition and Casting: Slight increases in Mg (0.92 %) and Si (1.09 %) content, combined with a higher casting speed ($120\,\mathrm{mm\,s^{-1}}$) and lower pouring temperature (699 °C), improved grain refinement and β'' precipitate formation, significantly boosting strength and ductility.

(3.) Cooling Benefits in Extrusion: Direct water shock cooling and nitrogen gas cooling during extrusion improved surface smoothness, hardness, and microstructural homogeneity while reducing die thermal fatigue, highlighting cooling as a critical factor in profile quality.

(4.) Microstructural Effects: Compared to 8 hours, longer homogenisation (10 hours) reduced shrinkage gaps and porosity. However, optimal mechanical properties were associated with smaller, more uniform grain sizes and ductile fracture surfaces, as observed in B2 and B3 via SEM analysis.

(5.) Anodizing Performance: Anodizing at 18 V for 32 minutes produced thicker (up to 11.7 µm) and glossier oxide layers, with surface quality linked to prior homogenisation and ageing processes, emphasizing their role beyond mechanical enhancement.

ACKNOWLEDGEMENTS

The authors would like to express their gratitude to Zahit Alüminyum and Sistem Alüminyum companies for supporting this paper.

REFERENCES

[1] A. Mozalev, A. Poznyak, I. Mozaleva, A. W. Hassel. The voltage-time behaviour for porous anodizing of aluminium in a fluoride-containing oxalic acid electrolyte. *Electrochemistry Communications* **3**(6):299–305, 2001. https://doi.org/10.1016/S1388-2481(01)00157-6

[2] Q. Li, J. O. Jensen, N. J. Bjerrum. Chemistry, electrochemistry, and electrochemical applications: Aluminum. In *Encyclopedia of Electrochemical Power Sources*, pp. 695–708. Elsevier, United Kingdom, 2009. https://doi.org/10.1016/B978-044452745-5.00951-5

[3] P. Schempp, C. E. Cross, C. Schwenk, M. Rethmeier. Influence of Ti and B additions on grain size and weldability of aluminium alloy 6082. *Welding in the World* **56**(9):95–104, 2012. https://doi.org/10.1007/BF03321385

[4] G. Mrówka-Nowotnik. Influence of chemical composition variation and heat treatment on microstructure and mechanical properties of 6XXX alloys. *Archives of Materials Science and Engineering* **46**(2):98–107, 2010.

[5] G. Mrówka-Nowotnik, J. Sieniawski. Influence of heat treatment on the microstructure and mechanical properties of 6005 and 6082 aluminium alloys. *Journal of Materials Processing Technology* **162–163**:367–372, 2005. https://doi.org/10.1016/j.jmatprotec.2005.02.115

[6] A. R. Prabhukhot, K. Prasad. Effect of heat treatment on hardness of 6082-T6 aluminum alloy. *International Journal of Scientific & Engineering Research* **6**(12):38–42, 2015.

[7] W. Ma, B. Wang, L. Yang, et al. Influence of solution heat treatment on mechanical response and fracture behaviour of aluminium alloy sheets: An experimental study. *Materials & Design* **88**:1119–1126, 2015. https://doi.org/10.1016/j.matdes.2015.09.044

[8] M. W. Meredith, J. Worth, R. Hamerton. Intermetallic phase selection during solidification of Al-Fe-Si(-Mg) alloys. In *Aluminium Alloys 2002 – ICAA8*, vol. 396–402 of *Materials Science Forum*, pp. 107–112. Trans Tech Publications Ltd, 2002. https://doi.org/10.4028/www.scientific.net/MSF.396-402.107

[9] G. Sha, K. O'Reilly, B. Cantor, et al. Effect of grain refiner on intermetallic phase formation in directional solidification of 6XXX series wrought Al alloys. In *Aluminium Alloys – Their Physical and Mechanical Properties*, vol. 331–337 of *Materials Science Forum*, pp. 253–258. Trans Tech Publications Ltd, 2000. https://doi.org/10.4028/www.scientific.net/MSF.331-337.253

[10] T. Tokarski. Thermo-mechanical processing of rapidly solidified 5083 aluminium alloy – structure and mechanical properties. *Archives of Metallurgy and Materials* **60**(1):177–180, 2015. https://doi.org/10.1515/amm-2015-0028

[11] P. K. Saha. Thermodynamics and tribology in aluminum extrusion. *Wear* **218**(2):179–190, 1998. https://doi.org/10.1016/S0043-1648(98)00210-5

[12] O. Engler, S. Miller-Jupp. Control of second-phase particles in the Al-Mg-Mn alloy AA5083. *Journal of Alloys and Compounds* **689**:998–1010, 2016. https://doi.org/10.1016/j.jallcom.2016.08.070

[13] P. S. Mohanty, J. E. Gruzleski. Mechanism of grain refinement in aluminium. *Acta Metallurgica et Materialia* **43**(5):2001–2012, 1995. https://doi.org/10.1016/0956-7151(94)00405-7

[14] O. Güven. *Structural analysis of Al-Si-Mg casting alloy*. Master's thesis, Istanbul Technical University, 2005.

[15] M. Şahbaz. Effect of artificial aging and cooling rate on microstructure and mechanical properties of AA6082. *European Journal of Science and Technology* (28):300–305, 2021. https://doi.org/10.31590/ejosat.998077

[16] T. Björk, R. Westergård, S. Hogmark. Wear of surface treated dies for aluminium extrusion – A case study. *Wear* **249**(3–4):316–323, 2001. https://doi.org/10.1016/S0043-1648(01)00550-6

[17] O. Olaseinde, B. Adewuyi. Effect of ceramic powder coatings on low carbon steel. *Materials Sciences and Applications* **7**(5):221–231, 2016. https://doi.org/10.4236/msa.2016.75022

[18] E. Cirik, K. Genel. Effect of anodic oxidation on fatigue performance of 7075-T6 alloy. *Surface and Coatings Technology* **202**(21):5190–5201, 2008. https://doi.org/10.1016/j.surfcoat.2008.06.049

[19] M. Ardelean, S. Lascău, E. Ardelean, A. Josan. Surface treatments for aluminium alloys. *IOP Conference Series: Materials Science and Engineering* **294**(1):012042, 2018. https://doi.org/10.1088/1757-899X/294/1/012042

[20] Y. Chen, A. H. Clausen, O. S. Hopperstad, M. Langseth. Stress-strain behaviour of aluminium alloys at a wide range of strain rates. *International Journal of Solids and Structures* **46**(21):3825–3835, 2009. https://doi.org/10.1016/j.ijsolstr.2009.07.013

[21] L. Djapic Oosterkamp, A. Ivankovic, G. Venizelos. High strain rate properties of selected aluminium alloys. *Materials Science and Engineering: A* **278**(1–2):225–235, 2000. https://doi.org/10.1016/S0921-5093(99)00570-5

[22] S. Jadhav, R. Singh, V. Pawar, S. Mane. Influence of heat treatment on mechanical properties and microstructure of EN AW 6082 aluminum alloy. In *2017 8th International Conference on Mechanical and Aerospace Engineering (ICMAE)*, pp. 184–187. 2017. https://doi.org/10.1109/ICMAE.2017.8038639